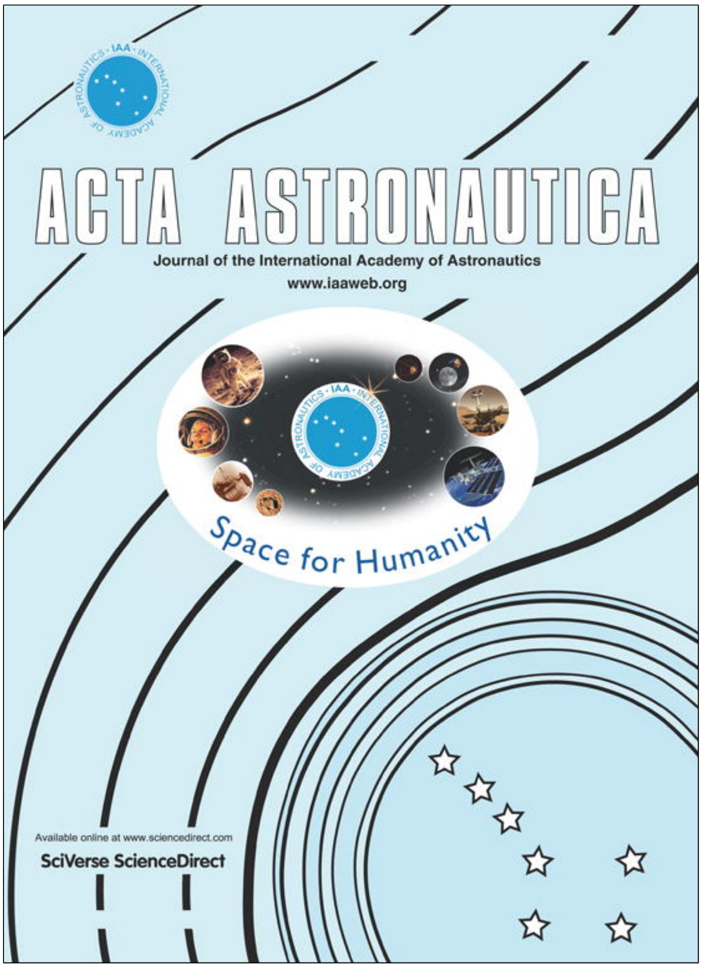
ACTA ASTRONAUTICA
Journal of the International Academy of Astronautics
www.iaaweb.org
Space for Humanity
Available online at www.sciencedirect.com
SciVerse ScienceDirect

Acta Astronautica 88 (2013) 89–97

Contents lists available at SciVerse ScienceDirect

Acta Astronautica

journal homepage: www.elsevier.com/locate/actaastro

Out-of-plane stability analysis of collinear spinning three-craft Coulomb formations

Peter D. Jasch *, Erik A. Hogan, Hanspeter Schaub

Aerospace Engineering Sciences Department, University of Colorado, Boulder, CO 80309-0431, USA

ARTICLE INFO

Article history:
Received 30 April 2012
Received in revised form
31 January 2013
Accepted 5 March 2013
Available online 16 March 2013

Keywords:
Formation flying
Coulomb formations
Stability analysis
Nonlinear control

ABSTRACT

The results of a stability analysis focusing on the out-of-plane motion of collinear three-craft Coulomb formations with set charges are discussed. Such a formation is assumed to be spinning in deep space without relevant gravitational forces present. Assuming in-plane motion only with circular relative trajectories and initial position and velocity perturbations confined to the orbital plane, the previous work analytically proves marginal stability in the linear sense and numerically shows marginal stability in the short term. In this paper, the equations of motion are presented in the cylindrical coordinate frame in order to analyze the out-of-plane motion in more detail. The out-of-plane motion is shown to decouple to first order from the marginally stable in-plane motion. A simple control law is developed and applied, which directly controls the out-of-plane motion only within specified deadbands. For a wide variety of out-of-plane perturbations, the control law succeeds in preserving the in-plane variant shape despite some out-of-plane motion. A trend between the settling time and deadband, which defines the largest out-of-plane errors allowed before the controller is turned on, is determined, which illustrates how large the deadband may be before the in-plane motion is affected.

1. Introduction

As the number of scientific missions venturing out into the Solar System and beyond increases, close formation flying of spacecraft proves to be the emerging technology that makes previously impossible missions become reality. With separation distances on the order of tens of meters, a formation of spacecraft may be used in applications in the fields of Earth imaging, advanced weather monitoring, planetary research, astronomy, and more [1]. Close-proximity spacecraft formations provide the freedom to place a large number of scientific instrumentation within a formation of satellites separated by tens of meters, rather than being limited to a fixed geometry and shape of a single satellite. Rather, the free-flying formation can morph into new sizes and shapes, providing the sensors a variable aperture. Furthermore, the satellites in the formation may be placed into orbit upon separate launch vehicles. If a budget or time constraint exists, this aspect proves to be an advantage. As a result, a formation of this sort may be built over a period of time.

Electrostatic actuation using active charge control has been proposed as early as 1966, where it was suggested as a means to inflate a membrane structure in geosynchronous orbit altitudes [2]. In such space regions the local plasma results in very low Watt-level electrical power requirements and low Debye shielding effects. Starting in 2002, Coulomb formations that are proposed use electrostatic forces to maintain the shape of the spacecraft formation [3–5]. Attractive and repulsive forces are generated when charging individual spacecraft within the formation [6]. For constellations of satellites flying in close

* Corresponding author. Tel.: +1 832 407 0743.
E-mail addresses: peter.jasch@colorado.edu (P.D. Jasch), erik.hogan@colorado.edu (E.A. Hogan), hanspeter.schaub@colorado.edu (H. Schaub).
URL: http://hanspeterschaub.info (H. Schaub).

0094-5765/$ - see front matter © 2013 IAA Published by Elsevier Ltd. All rights reserved.
http://dx.doi.org/10.1016/j.actaastro.2013.03.005

proximity, on the order of tens of meters, small thrust levels on the order of micro-Newtons are needed from the propulsion system for formation maintenance. Furthermore, since sensitive scientific instruments onboard the satellites can easily be contaminated by caustic exhaust from traditional propellant-type thrusters, an electrostatic control system provides a means to control the spacecraft formation shape free from exhaust particles. As an active control system, it is very energy efficient in geosynchronous and deep space regions, requiring power levels on the order of Watts [7,8]. Active spacecraft charge control in space has been demonstrated on multiple missions [9,10], but to date it has not been employed for direct relative motion control.

The current study considers collinear spinning three-craft invariant shape Coulomb formations in deep space as the spacecraft orbits about their collective center of mass in circular trajectories. This formation is depicted in Fig. 1. Hussein and Schaub provide the theoretical foundation for determining invariant shape solutions for the three-craft Coulomb formation [11]. By specifying the craft charges, the collinear shape of the formation can be determined. Hogan and Schaub view the problem from a mission design perspective and solve for the craft charges when the collinear shape of the formation is specified [12]. It is proven that for any desired collinear invariant shape geometry, there exists a real charge solution. In fact, it is possible for up to three invariant shape solutions to exist for a single set of craft charges [13]. Through linear stability analysis, Ref. [13] demonstrates that the in-plane motion may be marginally stable for the three-craft invariant shape formations in circular trajectories if particular formation geometries are selected. This marginal stability is strictly in the linear sense and only observed when two invariant shape solutions exist for a set of craft charges [13]. One of these solutions is found to have unstable in-plane motion, while the other numerically exhibits marginally stable rotational motion in the short term. This marginally stable configuration is a significant find in which it greatly simplifies the charged relative motion control of the three bodies. Earlier work only identified strongly unstable charged collinear configurations [14,15]. Further, prior to Ref. [13], the only other passively stable charged relative motion configuration was the spinning charged two-body system discussed in Ref. [16].

The study of invariant shape Coulomb formations is a special case of the more general charged three-body problem, which is, itself, an extension of the classical gravitational three-body problem as discussed in Refs. [7,17,18]. Typically, the charged three-body problem considers the combined effects of gravitational and electrostatic forces on the motion of the bodies in the system. In the special case of invariant shape Coulomb formations, the relatively small masses of the bodies (100s of kg) result in gravitational forces many orders of magnitude below the electrostatic forces. The lack of significant gravitational forces is actually a limitation on the system, as fewer forces are available to stabilize a relative geometry. In Ref. [17], for example, a non-planar relative equilibrium is made possible by the combined influence of gravity and electrostatics. In Ref. [18], central configurations are identified for the charged three-body problem. Stability of these central configurations is investigated in Ref. [17].

In the current study, the charged three-body problem is considered for the case where the masses are too small to contribute meaningful gravitational forces. That is, only electrostatic forces are assumed to be acting on the bodies in the system. Collinear central configurations are the focus, where the craft orbits the center of mass of the formation on circular trajectories. The effects of motion outside this orbit plane are considered, with attention paid to resulting instabilities. In order to build upon the previously defined results in Refs. [12,13], we determine if this out-of-plane motion decouples from the in-plane motion. If this is the case, then it is likely that small out-of-plane perturbations will not destabilize the in-plane motion until the magnitude of these perturbations becomes significant. This paper investigates a simple control strategy to keep the out-of-plane motion within a small enough deadband such that the out-of-plane motion does not couple into the in-plane motion and destabilize the collinear central configuration.

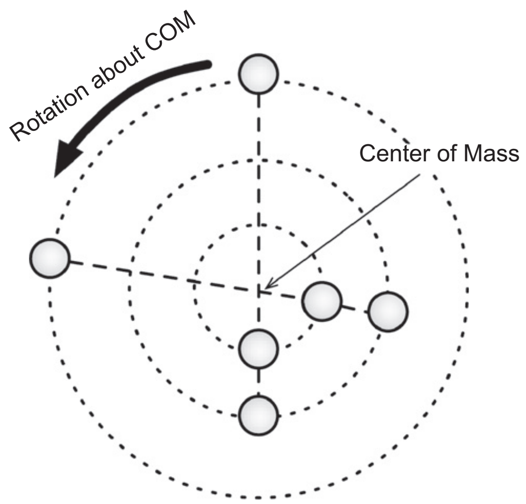

Fig. 1. Collinear three-craft invariant shape Coulomb formation.

2. Invariant shape solutions of Coulomb formations

The dynamic behavior of collinear invariant shape three-craft Coulomb formations is investigated. A sample formation is illustrated in Fig. 2. The three craft rotate about their center of mass in deep space. Similar to work done by Refs. [11,13], by assuming nonexistent gravitational forces and perturbations, the only forces which the spacecraft experience are due to the inter-craft electrostatic forces.

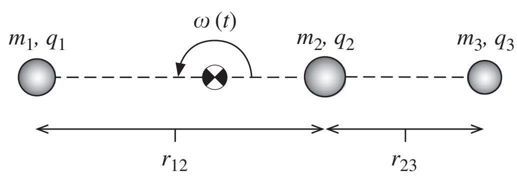

Fig. 2. Collinear invariant shape Coulomb formation [12].

The spacecraft are of mass m_i and charge q_i. For an invariant shape solution describing the formation geometry, the craft charges are assumed constant for all time. Each spacecraft has a position vector which describes the craft's location relative to the formation center of mass and is denoted by $\boldsymbol{r}_i$. The relative position vectors between spacecraft i and spacecraft j are denoted by $\boldsymbol{r}_{ij}=\boldsymbol{r}_j-\boldsymbol{r}_i$. An invariant shape Coulomb formation does not imply a fixed shape, as in constant inter-craft distances and constant distances between each craft and the center of mass. Rather, an invariant shape Coulomb formation implies a constant ratio of inter-craft distances. This is made apparent by consideration of the collinear formation as depicted in Fig. 2. As the craft orbits about the center of mass, the separation distances between the craft are allowed to vary as long as the ratio of the separation distances, χ, remains constant

$$\chi=\frac{r_{23}}{r_{12}}. \tag{1}$$

It is important to note that χ will always be positive due to positive separation distances between the spacecraft. As the spacecraft orbits about the formation center of mass, they follow Keplerian trajectories with time-varying angular velocities, $\omega(t)$ [11]. The trajectories of the spacecraft may be circular, elliptic, parabolic, or hyperbolic while maintaining a collinear formation for all time.

In order to maintain an invariant shaped Coulomb formation, the three craft must possess specific charges. These charges are a function of the formation geometry and angular momentum (i.e. craft masses, craft angular velocity, and inter-craft separation distances). Thus, by specifying a set of craft charges, Hussein and Schaub [11] prove that the collinear formation geometry, χ, may be found by solving a modified form of Lagrange's quintic equation.

For initial analysis, a deep-space plasma condition is assumed, where the effective Debye length is sufficiently large to make the plasma-related charge shielding negligible. Because the spacecraft potentials are relatively large with respect to the plasma temperatures, effective Debye lengths [19] must be considered which are multiple times those of regular, low-potential Debye lengths. For example, in GEO the effective Debye lengths can be 3–5 times larger if the craft is charged to 10s of kilo-Volts. Thus, a deep space Debye length of 25 m would act, from a force perspective, like an effective Debye length closer to 100 m [20]. Thus, considering the effective Debye lengths with large potentials, the assumption of negligible Debye shielding for this three-craft formation flying dozens of meters apart is warranted.

By specifying the craft charges and masses, a total of six parameters, it is possible to determine solutions for χ. In real-world applications, a Coulomb formation mission would most likely be designed by specifying the formation geometry, and then solving for the necessary craft charges as they are functions of the Coulomb formation geometry. This method requires the craft masses, formation spin rate, and χ to be specified. Once these parameters are specified, the craft charges are then solved for. The quintic equation used allows for either methods to be performed. By assuming that the three craft are is of equal mass, m, and the Coulomb formation is operating in a space environment with large effective Debye lengths, the quintic equation can be simplified. To do this, the craft charge ratios are first introduced as

$$\delta=\frac{q_1}{q_3},\quad \sigma=\frac{q_1}{q_2}. \tag{2}$$

These charge ratios allow the craft charges to be determined after one craft charge is assumed. From these definitions and assumptions, the quintic equation simplifies to

$$0=-2-5\chi+(\delta-\sigma-4)\chi^2+(4\delta+\sigma-1)\chi^3+5\delta\chi^4+2\delta\chi^5. \tag{3}$$

The six total parameters from the original quintic equation are reduced to two, δ and σ. Ref. [13] examines the craft charge solution space in detail to find δ and σ values, which yield multiple invariant shape solutions, χ.

To illustrate the concept of multiple invariant shape solutions in numerical results, Ref. [13] uses charge ratios of $\delta=-0.05$ and $\sigma=7$. This solution leads to two positive real roots of the quintic equation, χ values which determine two invariant shape solutions for Coulomb formations, $\chi=3.2508$ and $\chi=4.3283$. A linear stability analysis is then conducted to determine which of these χ solutions produce a stable spacecraft formation. It is found that the χ value of 3.2508 corresponds to an equilibrium numerically exhibiting marginal stability in the short term while the χ value of 4.3283 results in an unstable invariant shape. The current study investigates the marginally stable solution, $\chi=3.2508$, in more detail in order to control the out-of-plane motion and create a stable spacecraft formation indefinitely.

3. Dynamical analysis

3.1. Cylindrical equations of motion

From derivations in Ref. [13], an inertial description of the spacecraft motion about the formation center of mass is

$$m_i\ddot{\boldsymbol{r}}_i=\boldsymbol{F}_i=\sum_{j=1,j\neq i}^{3}k_c\frac{q_iq_j}{r_{ij}^2}\hat{\boldsymbol{e}}_{\boldsymbol{ji}}, \tag{4}$$

where $k_c=8.99\times10^9\ \mathrm{Nm/C^2}$ is the Coulomb constant, q_i and q_j are the charges of crafts i and j, respectively, r_{ij} is the distance between the crafts i and j, and $\hat{\boldsymbol{e}}_{\boldsymbol{ji}}$ is the unit vector from craft j to craft i. In order to gain further insight into the motion of collinear invariant shape Coulomb formations, the previously stated inertial equations of motion are derived in a cylindrical coordinate frame. This process begins by presenting the position vectors of each spacecraft in the Coulomb formation with respect to a cylindrical coordinate frame. The position of each craft is defined by a radius magnitude, r_i, representing the planar distance from the formation center of mass to the current craft i, an angle, θ_i, specifying the rotation between the inertial $\hat{\boldsymbol{e}}_1$ axis and the craft radius vector at the current time, and an out-of-plane component, z_i. In the cylindrical frame, the position of a craft i in the formation is given by

$$\boldsymbol{R}_i = [r_i \cos(\theta_i) \ \ r_i \sin(\theta_i) \ \ z_i]. \tag{5}$$

The acceleration expression in Eq. (4) is used to obtain the new equations of motion, which require differentiation of Eq. (5) in order to obtain $\ddot{r}_i$ for each craft. After carrying out the required differentiation and substitution into Eq. (4), the equations of motion in cylindrical coordinates are

$$\ddot{r}_1 = \frac{k_c q_1 (r_1(q_2 r_{13}^3 + q_3 r_{12}^3) - q_2 r_{13}^3 r_2 \cos(\theta_1-\theta_2) - q_3 r_{12}^3 r_3 \cos(\theta_1-\theta_3))}{m_1 r_{12}^3 r_{13}^3} + r_1 \dot{\theta}_1^2 \tag{6a}$$

$$\ddot{r}_2 = \frac{k_c q_2 (q_1 r_{23}^3 (r_2 - r_1 \cos(\theta_1-\theta_2)) + q_3 r_{12}^3 (r_2 - r_3 \cos(\theta_2-\theta_3)))}{m_2 r_{12}^3 r_{23}^3} + r_2 \dot{\theta}_2^2 \tag{6b}$$

$$\ddot{r}_3 = \frac{k_c q_3 (q_1 r_{23}^3 (r_3 - r_1 \cos(\theta_1-\theta_3)) + q_2 r_{13}^3 (r_3 - r_2 \cos(\theta_2-\theta_3)))}{m_3 r_{13}^3 r_{23}^3} + r_3 \dot{\theta}_3^2 \tag{6c}$$

$$\ddot{\theta}_1 = k_c q_1 \left(\frac{q_2 r_2 \sin(\theta_1-\theta_2)}{m_1 r_1 r_{12}^3} + \frac{q_3 r_3 \sin(\theta_1-\theta_3)}{m_1 r_1 r_{13}^3} \right) - \frac{2\dot{r}_1 \dot{\theta}_1}{r_1} \tag{6d}$$

$$\ddot{\theta}_2 = k_c q_2 \left(\frac{q_3 r_3 \sin(\theta_2-\theta_3)}{m_2 r_2 r_{23}^3} + \frac{q_1 r_1 \sin(\theta_1-\theta_2)}{m_2 r_2 r_{12}^3} \right) - \frac{2\dot{r}_2 \dot{\theta}_2}{r_2} \tag{6e}$$

$$\ddot{\theta}_3 = -k_c q_3 \left(\frac{q_1 r_1 \sin(\theta_1-\theta_3)}{m_3 r_3 r_{13}^3} + \frac{q_2 r_2 \sin(\theta_2-\theta_3)}{m_3 r_3 r_{23}^3} \right) - \frac{2\dot{r}_3 \dot{\theta}_3}{r_3} \tag{6f}$$

$$\ddot{z}_1 = k_c q_1 \left(\frac{q_2 (z_1 - z_2)}{m_1 r_{12}^3} + \frac{q_3 (z_1 - z_3)}{m_1 r_{13}^3} \right) \tag{6g}$$

$$\ddot{z}_2 = k_c q_2 \left(\frac{q_1 (z_2 - z_1)}{m_2 r_{12}^3} + \frac{q_3 (z_2 - z_3)}{m_2 r_{23}^3} \right) \tag{6h}$$

$$\ddot{z}_3 = k_c q_3 \left(\frac{q_1 (z_3 - z_1)}{m_3 r_{13}^3} + \frac{q_2 (z_3 - z_2)}{m_3 r_{23}^3} \right). \tag{6i}$$

3.2. Linearization of cylindrical equations of motion

Ref. [13] numerically proves the Coulomb formation in-plane motion to be marginally stable in the short term for a specified set of formation parameters χ, δ, and σ. The in-plane motion of the Coulomb formation preserves its shape while the out-of-plane motion remains relatively small compared to the formation geometry. From this observation, it is hypothesized that the out-of-plane motion decouples from the in-plane motion for small deviations from the reference. To prove this hypothesis, the newly developed cylindrical equations of motion are linearized. The equations of motion for the in-plane motion, $\boldsymbol{r}$ and $\boldsymbol{\theta}$, and out-of-plane motion, $\boldsymbol{z}$, are described in Eq. (6) and are written as

$$\boldsymbol{f}_r(\boldsymbol{r},\boldsymbol{\theta},\boldsymbol{z}) = \begin{bmatrix} \ddot{r}_1 \\ \ddot{r}_2 \\ \ddot{r}_3 \end{bmatrix}, \quad \boldsymbol{f}_\theta(\boldsymbol{r},\boldsymbol{\theta},\boldsymbol{z}) = \begin{bmatrix} \ddot{\theta}_1 \\ \ddot{\theta}_2 \\ \ddot{\theta}_3 \end{bmatrix}, \quad \boldsymbol{f}_z(\boldsymbol{r},\boldsymbol{\theta},\boldsymbol{z}) = \begin{bmatrix} \ddot{z}_1 \\ \ddot{z}_2 \\ \ddot{z}_3 \end{bmatrix} \tag{7}$$

A reference state, $(\boldsymbol{r}_r, \boldsymbol{\theta}_r, \boldsymbol{z}_r)$, must first be established, which the equations of motion are linearized about. For a stable formation, the out-of-plane positions, velocities, and accelerations are zero, i.e. $\boldsymbol{z}_r = \dot{\boldsymbol{z}}_r = \ddot{\boldsymbol{z}}_r = 0$. For the in-plane reference motion, the radial positions are constant with zero velocities and accelerations, i.e. $\boldsymbol{r}_r = [r_1 \ r_2 \ r_3]^T$ and $\dot{\boldsymbol{r}}_r = \ddot{\boldsymbol{r}}_r = 0$. While invariant shape Coulomb formations can have elliptical or circular trajectories, this linearization is about circular trajectories where the spacecraft separations are constant. Also, the two craft on the same side of the center of mass have an angular position $\pm\pi$ radians of the third craft and the angular rates of all three craft are constant with zero acceleration, i.e. $\theta_r = \theta_1 = \theta_2$, $\theta_3 = \theta_r \pm \pi$, $\dot{\theta}_r = \dot{\theta}_1 = \dot{\theta}_2 = \dot{\theta}_3$, and $\ddot{\theta}_r = \ddot{\theta}_1 = \ddot{\theta}_2 = \ddot{\theta}_3 = 0$. The tracking errors, $\Delta\boldsymbol{r}$, $\Delta\boldsymbol{\theta}$, and $\Delta\boldsymbol{z}$, describe the residuals from the current state to the reference state, which the Coulomb formation out-of-plane motion is being driven to.

The in-plane and out-of-plane equations of motion from Eq. (7) are then linearized about the reference trajectory using a Taylor series expansion and dropping higher-order terms. This gives the result

$$\boldsymbol{f}(\boldsymbol{r},\boldsymbol{\theta},\boldsymbol{z}) \approx \left.\frac{\partial \boldsymbol{f}(\boldsymbol{r},\boldsymbol{\theta},\boldsymbol{z})}{\partial \boldsymbol{r}}\right|_{\boldsymbol{r}=\boldsymbol{r}_r} \Delta\boldsymbol{r} + \left.\frac{\partial \boldsymbol{f}(\boldsymbol{r},\boldsymbol{\theta},\boldsymbol{z})}{\partial \boldsymbol{\theta}}\right|_{\boldsymbol{\theta}=\boldsymbol{\theta}_r} \Delta\boldsymbol{\theta} + \left.\frac{\partial \boldsymbol{f}(\boldsymbol{r},\boldsymbol{\theta},\boldsymbol{z})}{\partial \boldsymbol{z}}\right|_{\boldsymbol{z}=\boldsymbol{z}_r} \Delta\boldsymbol{z}, \tag{8}$$

where $\boldsymbol{f}$ is the combination of $\boldsymbol{f}_r$, $\boldsymbol{f}_\theta$, and $\boldsymbol{f}_z$ from Eq. (7). The first order sensitivities of $\boldsymbol{f}_z$ with respect to the states $\boldsymbol{r}$ and $\boldsymbol{\theta}$ are zero. This result is due to the linearization about $z_1 = z_2 = z_3 = 0$. The partials of $\boldsymbol{f}_z$ with respect to r are linear functions of z. Since the formation equilibrium is defined by the spacecraft moving in circular trajectories, these terms evaluate to 0. Then, the out-of-plane $\boldsymbol{z}$ motion decouples to first order from the in-plane motion since the sensitivities of $\boldsymbol{f}_r$ and $\boldsymbol{f}_\theta$ with respect to $\boldsymbol{z}$ are zero

$$\left.\frac{\partial \boldsymbol{f}_z(\boldsymbol{r},\boldsymbol{\theta},\boldsymbol{z})}{\partial \boldsymbol{r}}\right|_{\boldsymbol{r}=\boldsymbol{r}_r} = \boldsymbol{0}, \quad \left.\frac{\partial \boldsymbol{f}_z(\boldsymbol{r},\boldsymbol{\theta},\boldsymbol{z})}{\partial \boldsymbol{\theta}}\right|_{\boldsymbol{\theta}=\boldsymbol{\theta}_r} = \boldsymbol{0} \tag{9}$$

The cylindrical coordinate system chosen provides a natural method to discuss the charged spinning three-craft motion. Next, it is of interest to determine if this out-of-plane motion is stable, and how large it must become before the higher order terms couple the in- and out-of-plane motions again. The linearized out-of-plane equations of motion are

$$f_z(\boldsymbol{r},\boldsymbol{\theta},\boldsymbol{z}) \approx [\boldsymbol{A}] \begin{bmatrix} z_1 \\ z_2 \\ z_3 \end{bmatrix} \tag{10a}$$

$$[\boldsymbol{A}(\boldsymbol{r}_r,\boldsymbol{\theta}_r,\boldsymbol{z}_r)] = \begin{bmatrix} \frac{k_c q_1}{m_1}\left(\frac{q_2}{r_{12}^3} + \frac{q_3}{r_{13}^3}\right) & -\frac{k_c q_1 q_2}{m_1 r_{12}^3} & -\frac{k_c q_1 q_3}{m_1 r_{13}^3} \\ -\frac{k_c q_1 q_2}{m_2 r_{12}^3} & \frac{k_c q_2}{m_2}\left(\frac{q_1}{r_{12}^3} + \frac{q_3}{r_{23}^3}\right) & -\frac{k_c q_2 q_3}{m_2 r_{23}^3} \\ -\frac{k_c q_1 q_3}{m_3 r_{13}^3} & -\frac{k_c q_2 q_3}{m_3 r_{23}^3} & \frac{k_c q_3}{m_3}\left(\frac{q_1}{r_{13}^3} + \frac{q_2}{r_{23}^3}\right) \end{bmatrix} \tag{10b}$$

Note that $[A]$ is fully populated, illustrating that while the $\boldsymbol{z}$ motion decouples from the $\boldsymbol{r}$ and θ motion, the individual z_i are still coupled. Further, the evaluation of $[A]$ depends on the equilibrium charges q_i of a particular configuration. For a given configuration, these charges are determined by solving Eq. (3), not a simple task to do analytically. Thus, the form of $[A]$ is not further reduced, and the following section performs a numerical study to investigate the out-of-plane stability.

3.3. Out-of-plane stability analysis

Ref. [13] defines a specific regime of δ and σ, which can be used to calculate two real roots of the quintic equation for collinear invariant shape Coulomb formations. For a stability analysis of the out-of-plane motion, an eigen decomposition is performed, which requires initial conditions for the formation. The initial Coulomb formation geometry parameters used in this paper are $\delta=-0.05$, $\sigma=7$, and $\chi=3.2508$. Table 1 lists the mass, m, the initial semi-major axis, r, the initial in-plane angle, θ, and charge, q, of each spacecraft within the Coulomb formation. The orbital period of all three craft is approximately 192 min.

This χ value of 3.2508 is one root of the quintic equation, which exhibits marginal stability for linearized in-plane motion only [13]. To analyze the stability of the out-of-plane dynamics, the linear equations of motion for the z-coordinates are considered. Because the system is second order, the z motion is described by

$$\begin{bmatrix} \Delta\dot{\boldsymbol{z}} \\ \Delta\ddot{\boldsymbol{z}} \end{bmatrix} = [B] \begin{bmatrix} \Delta\boldsymbol{z} \\ \Delta\dot{\boldsymbol{z}} \end{bmatrix}, \tag{11}$$

where

$$[B] = \begin{bmatrix} \mathbf{0} & \boldsymbol{I}_{3\times3} \\ [\boldsymbol{A}(\boldsymbol{r}_r,\boldsymbol{\theta}_r,\boldsymbol{z}_r)] & \mathbf{0} \end{bmatrix}. \tag{12}$$

The eigenvalues of the $[B]$ matrix provide information about the stability of the out-of-plane motion. Here, the conditions listed in Table 1 are used to populate the $[B]$ matrix. Recall that these initial conditions correspond to the $\chi=3.2508$ invariant shape, which is found to be marginally stable in the linear sense when only in-plane motion is considered [13]. The resulting eigenvalues of the $[B]$ matrix are $\pm 5.5i\times10^{-4}$, $\pm 2.8\times10^{-4}$, 0.0, and 0.0. The existence of a positive real number eigenvalue indicates that the out-of-plane motion is unstable. That is, any small departure from the nominal $\boldsymbol{z}=\dot{\boldsymbol{z}}=0$ will result in large deviations. Eventually, the z motion will grow large enough to couple back into the in-plane dynamics and degrade the shape. As long as the departures are small enough, however, the decoupling of the z-motion from the planar motion allows the formation shape to be maintained. In this regime, the out-of-plane motion does not affect the in-plane motion to first order.

This marginally stable root, in the linear sense, is shown to preserve the formation in-plane motion in the short term while the out-of-plane motion remains relatively small compared to the geometry of the Coulomb formation. An example of this behavior is presented next. By initializing the out-of-plane position of crafts 1 and 3 to be zero and perturbing craft 2 with an initial value of 0.001 m, the uncontrolled Coulomb formation slowly degrades and eventually collapses. Fig. 3 shows a three-dimensional view of the simulated full nonlinear formation dynamics over a few orbital periods. In this figure, the in-plane position has been projected down to the $z=-100$ m plane in order to visualize the formation degradation while the out-of-plane errors grow. While the out-of-plane errors grow to 10 or 20 m, the planar invariant-shape is preserved.

Table 1
Initial spacecraft parameters.

Craft	m (kg)	r (m)	θ (rad)	q (μC)
1	100	44.616	π	10
2	100	19.125	π	1.429
3	100	63.741	0	−200

While the out-of-plane errors are relatively small, it is acceptable to approximate the higher order terms in the equations of motion to be zero. As a result, the governing motion is described by the linearized equations of motion in Eq. (10). As the out-of-plane errors grow, the higher order terms grow and the in-plane motion is coupled with the out-of-plane motion. By controlling the out-of-plane motion to or near zero, the higher order terms are approximately equal to zero and the in-plane motion is decoupled from the out-of-plane motion. This simple controller that maintains small out-of-plane errors preserves the shape of the Coulomb formation.

3.4. Nonlinear controller development for out-of-plane motion

As previously stated, the Coulomb formation retains shape within the plane for small out-of-plane deviations. For this reason, the out-of-plane motion of the three craft is controlled in this paper to produce a stable Coulomb formation. This is a nonlinear controller which utilizes the nonlinear equations of motion for the out-of-plane motion described in Eq. (7).

By adding the controller for the out-of-plane motion, $\boldsymbol{u}_z$, the system now looks like

$$\ddot{\boldsymbol{z}} = \boldsymbol{f}(\boldsymbol{r},\boldsymbol{\theta},\boldsymbol{z})+\boldsymbol{u}_z. \tag{13}$$

It is assumed that a relative motion equilibrium has been chosen such that the in-plane motion $(\boldsymbol{r},\boldsymbol{\theta})$ is marginally stable in the linear sense. The following control does not

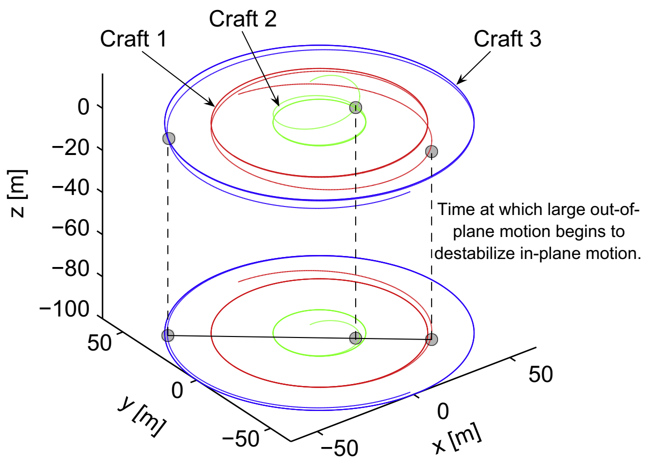

Fig. 3. Illustration of uncontrolled Coulomb formation dynamics with marginally stable in-plane motion.

control these states directly, but assumes that they are measurable. Lyapunov's Direct Method [21] is used in this paper to design a nonlinear controller and prove Lyapunov stability for the out-of-plane motion. This method requires the use of a scalar, energy-like Lyapunov function. The Lyapunov function for this analysis is

$$V(\Delta \boldsymbol{z}, \Delta \dot{\boldsymbol{z}}) = \frac{1}{2} \Delta \boldsymbol{z}^T [\boldsymbol{K}_1] \Delta \boldsymbol{z} + \frac{1}{2} \Delta \dot{\boldsymbol{z}}^T \Delta \dot{\boldsymbol{z}}, \tag{14}$$

where $[\boldsymbol{K}_1]$ is a symmetric, positive-definite matrix. In order for the out-of-plane motion to be Lyapunov stable, $V(\Delta \boldsymbol{z}, \Delta \dot{\boldsymbol{z}})$ is required to have continuous partial derivatives and be a positive definite function about the reference trajectory $\boldsymbol{z}_r$.

A third constraint for Lyapunov stability requires the Lyapunov function rate, $\dot{V}(\Delta \boldsymbol{z}, \Delta \dot{\boldsymbol{z}})$, to be negative semi-definite. The Lyapunov function rate is found by taking the time derivative of the Lyapunov function in Eq. (14).

$$\dot{V}(\Delta \boldsymbol{z}, \Delta \dot{\boldsymbol{z}}) = \Delta \dot{\boldsymbol{z}}^T [\Delta \ddot{\boldsymbol{z}} + [\boldsymbol{K}_1] \Delta \boldsymbol{z}] \tag{15}$$

To ensure that the Lyapunov function rate is negative semi-definite, the bracketed term in Eq. (15) is set equal to $-[\boldsymbol{K}_2]\Delta \dot{\boldsymbol{z}}$, where $[\boldsymbol{K}_2]$ is a symmetric, positive, definite matrix, so that

$$\dot{V}(\Delta \boldsymbol{z}, \Delta \dot{\boldsymbol{z}}) = -\Delta \dot{\boldsymbol{z}}^T [\boldsymbol{K}_2] \Delta \dot{\boldsymbol{z}} \le 0 \tag{16}$$

The Lyapunov function rate is only negative semi-definite and not negative definite because $V(\Delta \boldsymbol{z}, \Delta \dot{\boldsymbol{z}})$ is both a function of the position and velocity tracking errors, $\Delta \boldsymbol{z}$ and $\Delta \dot{\boldsymbol{z}}$, and the position tracking error $\Delta \boldsymbol{z}$ is not explicitly present within the $\dot{V}$ expression. The out-of-plane motion is now proven to be Lyapunov stable with the controller, $\boldsymbol{u}_z$, implemented. The controller can be solved for by setting the bracketed term in Eq. (15) equal to $-[\boldsymbol{K}_2]\Delta \dot{\boldsymbol{z}}$. Remembering that the reference trajectory is zero, $\boldsymbol{z}_r = \dot{\boldsymbol{z}}_r = \ddot{\boldsymbol{z}}_r = 0$, the controller which produces a Lyapunov stable out-of-plane motion is

$$\boldsymbol{u}_z = -\boldsymbol{f}(\boldsymbol{r}, \boldsymbol{\theta}, \boldsymbol{z}) - [\boldsymbol{K}_1] \Delta \boldsymbol{z} - [\boldsymbol{K}_2] \Delta \dot{\boldsymbol{z}}. \tag{17}$$

While the out-of-plane motion is proven to be Lyapunov stable, it is also proven to exhibit asymptotic stability through the use of the theorem developed by Mukherjee and Chen [22]. Taking higher order derivatives of the Lyapunov function and evaluating them on the set $\Delta \dot{\boldsymbol{z}} = 0$, the first non-zero derivative is found to be

$$\dddot{V}(\Delta \dot{\boldsymbol{z}} = 0) = -2 \Delta \boldsymbol{z}^T [K_1]^T [\boldsymbol{K}_2][K_1] \Delta \boldsymbol{z}. \tag{18}$$

Note that this is negative definite in terms of $\Delta \boldsymbol{z}$, proving asymptotic stability.

4. Numerical performance study

Due to the decoupling of the in-plane and out-of-plane motion to the first order of the collinear spinning three-craft Coulomb formation, the shape of the formation degrades as the out-of-plane spacecraft position errors grow. For small errors, relative to the formation geometry, the formation shape is preserved. A logical conclusion is to control the out-of-plane spacecraft position errors to the linear region where the in-plane and out-of-plane motions are isolated. A numerical performance study is conducted in order to analyze the integrity of the formation and determine the validity of applying the nonlinear controller, derived in the previous section, to the out-of-plane spacecraft motion and maintain a stable formation. The goal of this controller implementation is not to induce stable planar motion; in the absence of out-of-plane displacements, these formations exhibit marginal stability in the linear sense. Rather, the control implementation is used to prevent sufficient out-of-plane displacements that would result in coupling between the in-plane and out-of-plane dynamics. It is this coupling that ultimately destabilizes and degrades the formation shape. The results of this study are presented in the following sections.

4.1. Application of nonlinear controller

The gains within the nonlinear controller of Eq. (17), $[\boldsymbol{K}_1]$ and $[\boldsymbol{K}_2]$, are found by critically damping the system with a damping coefficient, ζ, of approximately one and choosing a settling time, T_s. Since the system behaves linearly when out-of-plane perturbations are small, the natural frequency, ω_n, and gains are calculated with Eqs.

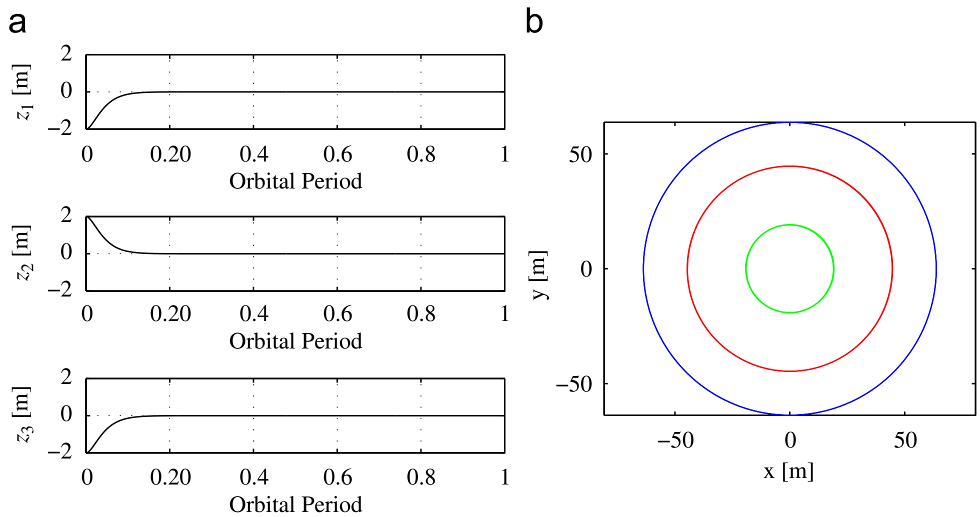

Fig. 4. Motion of controlled Coulomb formation. (a) Out-of-plane and (b) in-plane.

(19) through (21) [23].

$$\omega_n = -\frac{\log 0.02\sqrt{1-\zeta^2}}{\zeta T_s} \tag{19}$$

$$[\boldsymbol{K}_1] = \omega_n^2 \boldsymbol{I}_{3\times3} \tag{20}$$

$$[\boldsymbol{K}_2] = 2\zeta\omega_n \boldsymbol{I}_{3\times3} \tag{21}$$

For a settling time of 1 h, $[\boldsymbol{K}_1] = 1.4966 \times 10^{-5}\boldsymbol{I}_{3\times3}$ and $[\boldsymbol{K}_2] = 7.7373 \times 10^{-3}\boldsymbol{I}_{3\times3}$, where $\boldsymbol{I}_{3\times3}$ is a diagonal identity matrix.

In order to illustrate the effects of implementing such a controller, a simulation is run with initial out-of-plane position perturbations for crafts 1, 2, and 3 of −2, 2, and −2 m, respectively. During this simulation, the out-of-plane positions for all three craft are driven to zero.

The numerical simulation integrates the full, coupled nonlinear equations of motion for the spacecraft cluster given in Eq. (4). The out-of-plane motion is plotted over time for all three craft on the left side of Fig. 4. For the same simulation, the right side of Fig. 4 shows the in-plane projection of the Coulomb formation. This simulation numerically proves it is possible to preserve a Coulomb formation for an extended period of time for some specific initial conditions.

The analysis continues by expanding the initial out-of-plane errors on each craft. A sweep of initial conditions is performed by starting one craft at a zero out-of-plane error and varying the out-of-plane errors of the other two craft. The same simulation from the above is run with these initial conditions while monitoring the formation's shape factor, χ. After running each case for ten orbital periods, the final formation χ value is compared to the initial χ value of 3.2508. The results from this sweep are presented in Fig. 5. An asterisk, $*$, is plotted for those cases which produce a χ difference of less than or equal to 2% over ten orbital periods. While these results illustrate limitations in the initial out-of-plane errors for the three craft, these results also show how this controller application provides a formation maintenance solution for a wide variety of initial conditions.

This result numerically illustrates the decoupling of the out-of-plane motion from the in-plane motion, validating the analytic analysis and linearization performed on the Coulomb formation dynamics. Further, it reinforces the notion of marginal stability in the planar sense, and illustrates that by maintaining out-of-plane motion, the

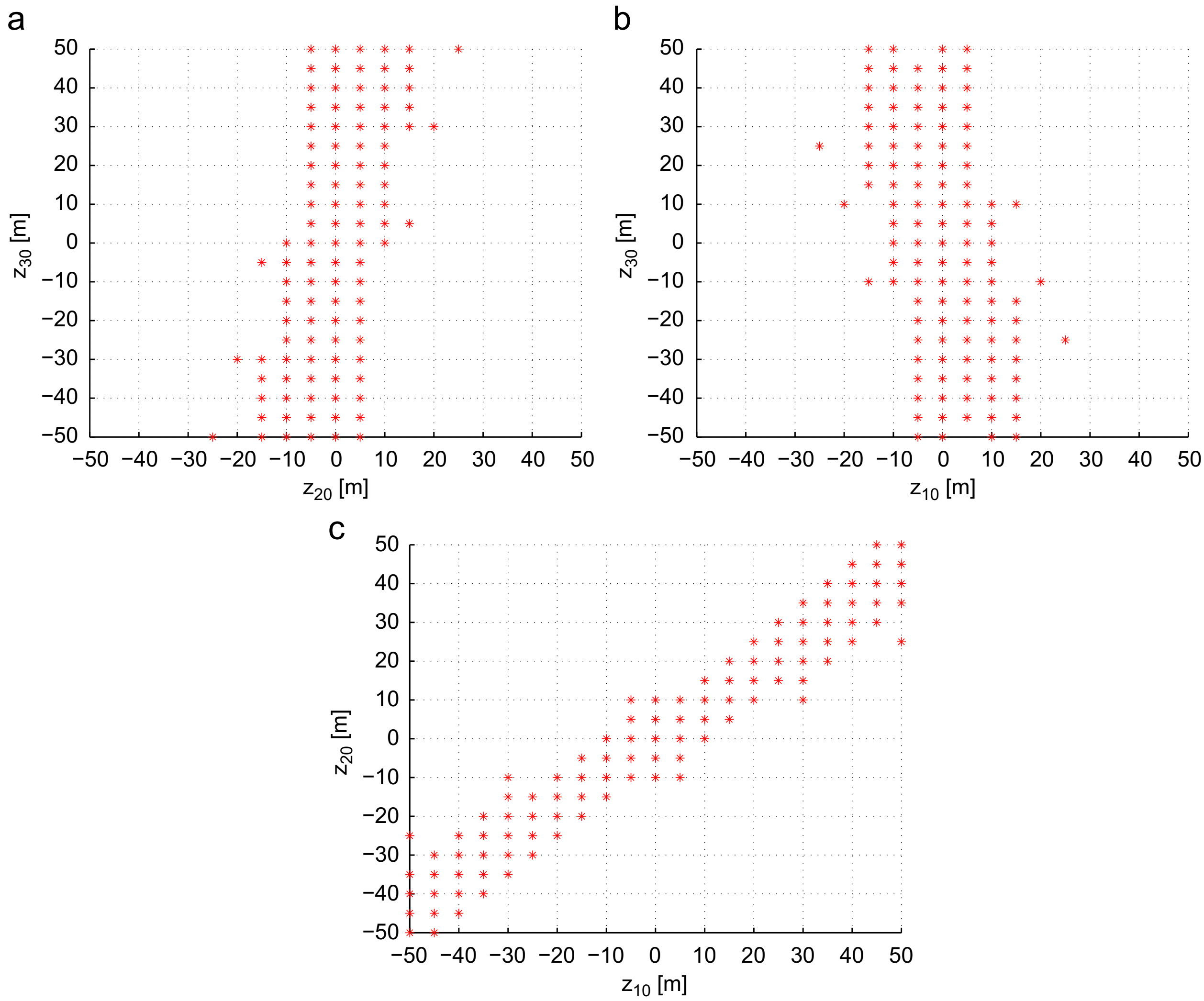

Fig. 5. Initial out-of-plane errors that preserve the formation shape within 2%. (a) $z_{1_0} = 0$, (b) $z_{2_0} = 0$, and (c) $z_{3_0} = 0$.

formation shape is preserved. Here, the full state is not being controlled, but only the out-of-plane direction (z). Thus, the formation can be maintained without full control of the system, reducing control requirements. By only controlling a portion of the state of the system, the formation maintenance is simplified.

4.2. Deadband analysis

In real applications, the out-of-plane errors may have some uncertainty due to sensor errors or model errors. To further examine this error uncertainty and the robustness of the Coulomb formation with the applied controller, a deadband is applied to the nonlinear controller. A deadband restricts the controller from working if the out-of-plane position error is less than a specified amount for any of the three craft. By adding this deadband and running the same simulations, the controller robustness is examined by modeling sensor errors within the system. For this new simulation, the initial out-of-plane perturbations are set to zero for crafts 1 and 3, while craft 2 is initialized at 0.001 m. This small error is implemented to cause the Coulomb formation to begin degrading. If all three craft are initialized at zero out-of-plane errors, the simulation would model an ideal case where the out-of-plane errors remain at a zero value. With a settling time of 1 h, the controller gains do not change. The simulation is run for ten orbital periods and the largest deadband to produce a stable Coulomb formation, to the nearest tenth of a meter, is ± 3.0 m. This value is determined through several numerical trial runs which incrementally increases the deadband by a tenth of a meter for each run until the Coulomb formation collapses. The out-of-plane motion for this case is depicted in the left side of Fig. 6 and the projected in-plane motion is shown on the right. These two graphs show that the Coulomb formation is preserved while the out-of-plane errors remain relatively small compared to the size of the formation.

By increasing the settling time to 8 h, the corresponding controller gains decrease to $[\boldsymbol{K}_1] = 2.3385 \times 10^{-7} \boldsymbol{I}_{3\times3}$ and $[\boldsymbol{K}_2] = 9.6716 \times 10^{-4} \boldsymbol{I}_{3\times3}$. With the same initial conditions as before, the largest deadband that maintains the in-plane shape decreases to ± 2.2 m. The out-of-plane and in-plane motions for this case are depicted in Fig. 7.

By varying the settling time and solving for the critically damped gains in the controller, a trend in the deadband is

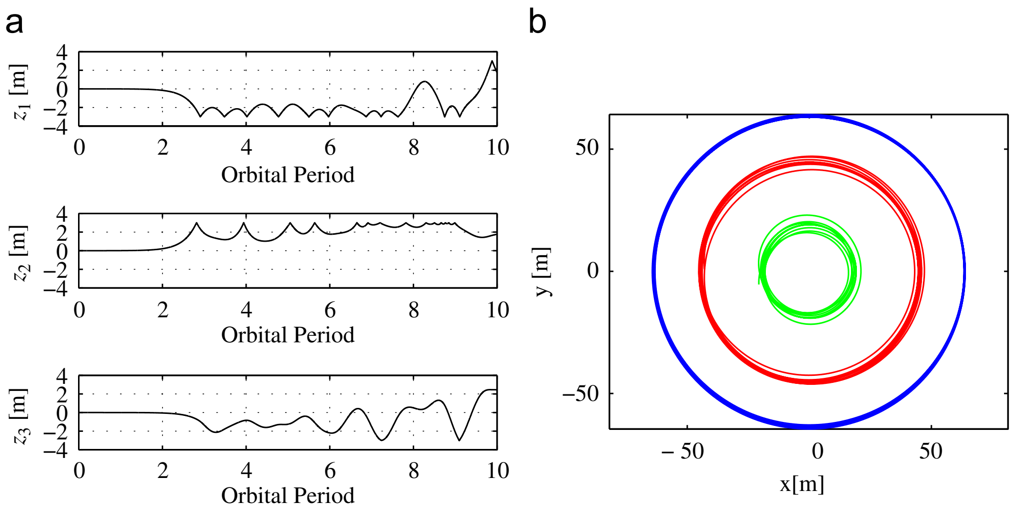

Fig. 6. Motion of controlled Coulomb formation with settling time of 1 h and a deadband of ± 3.0 m. (a) Out-of-plane and (b) in-plane.

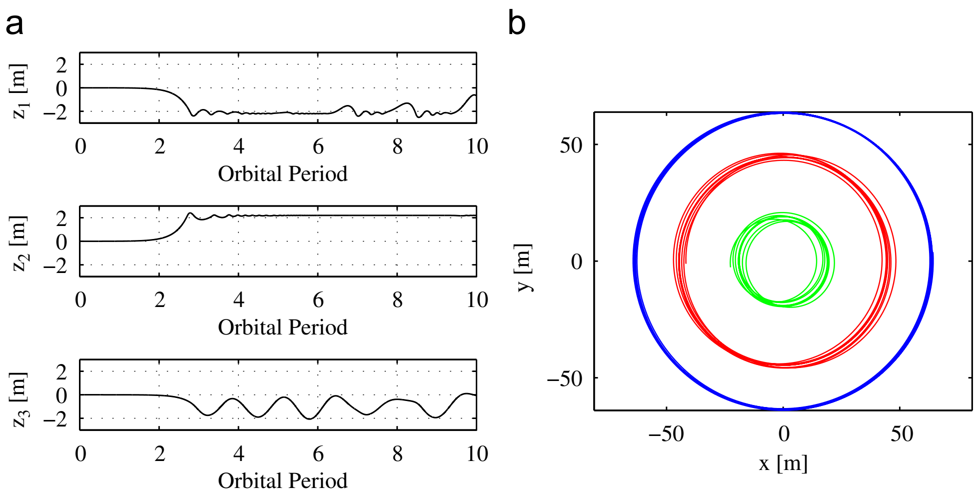

Fig. 7. Motion of controlled Coulomb formation with settling time of 8 h and a deadband of ± 2.2 m. (a) Out-of-plane and (b) in-plane.

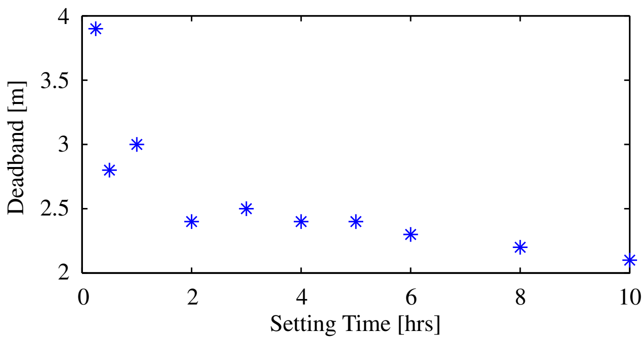

Fig. 8. Relationship between system settling time and maximum deadband width.

found. Fig. 8 shows the data collected from such an analysis. As the settling time increases, the largest allowable deadband decreases. This is due to a smaller force applied to the spacecraft by the controller. With a shorter settling time, the gains within the controller are larger and produce a larger force. This allows the out-of-plane motion to vary more, thus producing a larger allowable deadband. This data seems to dictate that there exists a deadband asymptote value; no matter how large the control input, the higher order terms in the out-of-plane motion will eventually degrade the in-plane shape of the formation.

5. Conclusion

By implementing a nonlinear controller for the out-of-plane motion the invariant-shape trajectories of the craft in the collinear formation are maintained in the presence of out-of-plane perturbations. The controller acts only on the out-of-plane motion, and is proven to be asymptotically stabilizing for a wide variety of initial out-of-plane errors. A deadband analysis provides a method to find the largest allowable out-of-plane error for a specified set of controller gains. Once the out-of-plane errors exceed this value, the controller is not able to preserve the Coulomb formation. By critically damping the system and varying the settling time, it is found that the largest allowable deadband is larger for shorter settling times. This is a result of larger forces produced by the controller. Prior research shows the in-plane motion to be stable [13], while the current research analyzes the instability of the out-of-plane motion, which compromises the Coulomb formation, and demonstrates how a simple control algorithm can be used to preserve the spacecraft formation indefinitely.

References

[1] P.R. Lawson, O. Lay, K.J. Johnston, C.A. Beichman, Terrestrial Planet Finder Interferometer Science Working Group, Technical Report JPL Publication 07-1, NASA Jet Propulsion Lab, 2007.

[2] J.H. Cover, W. Knauer, H.A. Maurer, Lightweight Reflecting Structures Utilizing Electrostatic Inflation, US Patent 3,526,706, 1966.

[3] L.B. King, G.G. Parker, S. Deshmukh, J.-H. Chong, Spacecraft Formation-flying using Inter-vehicle Coulomb Forces, Technical Report, NASA/NIAC, ⟨http://www.niac.usra.edu⟩, January 2002.

[4] L.B. King, G.G. Parker, S. Deshmukh, J.-H. Chong, Study of interspacecraft Coulomb forces and implications for formation flying, AIAA J. Propul. Power 19 (2003) 497–505.

[5] H. Schaub, G.G. Parker, L.B. King, Challenges and prospect of Coulomb formations, J. Astronaut. Sci. 52 (2004) 169–193.

[6] L. Pettazzi, D. Izzo, S. Theil, Swarm navigation and reconfiguration using electrostatic forces, in: 7th International Conference on Dynamics and Control of Systems and Structures in Space, The Old Royal Naval College, Greenwich, London, England.

[7] D.D. Dionysiou, G.G. Stamou, Stability of motion of the restricted circular and charged three-body problem, Astrophys. Space Sci. 152 (1989).

[8] C.R. Seubert, H. Schaub, Tethered Coulomb structures: prospects and challenges, J. Astronaut. Sci. 57 (2009) 347–368.

[9] E.G. Mullen, M.S. Gussenhoven, D.A. Hardy, Scatha survey of high-voltage spacecraft charging in sunlight, J. Geophys. Sci. 91 (1986) 1074–1090.

[10] H.B. Garrett, D.C. Schwank, S.E. DeFrost, A statistical analysis of the low energy geosynchronous plasma environment. I. Protons, Planet. Space Sci. 29 (1981) 1045–1060.

[11] I.I. Hussein, H. Schaub, Stability and control of relative equilibria for the three-spacecraft Coulomb tether problem, Acta Astronaut. 65 (2009) 738–754.

[12] E. Hogan, H. Schaub, Collinear invariant shapes for three-craft Coulomb formations, Acta Astronaut. 12 (2012) 78–89.

[13] E. Hogan, H. Schaub, Linear stability and shape analysis of spinning three-craft Coulomb formations, Celest. Mech. Dyn. Astron. 112 (2012) 131–148.

[14] I.I. Hussein, H. Schaub, Invariant shape solutions of the spinning three craft Coulomb tether problem, Celest. Mech. Dyn. Astron. 96 (2006) 137–157.

[15] S. Wang, H. Schaub, Coulomb control of nonequilibrium fixed shape triangular three-vehicle cluster, AIAA J. Guid. Control Dyn. 34 (2011) 259–270.

[16] H. Schaub, I.I. Hussein, Stability and reconfiguration analysis of a circulary spinning 2-craft Coulomb tether, IEEE Trans. Aerosp. Electron. Syst. 46 (2010) 1675–1686.

[17] F. Alfaro, E. Perez-Chavela, Linear stability of relative equilibria in the charged three-body problem, J. Diff. Eq. 245 (2008).

[18] E. Perez-Chavela, D.G. Saari, A. Susin, Z. Yan, Central configurations in the charged three body problem, Contemp. Math. 198 (1995).

[19] N. Murdoch, D. Izzo, C. Bombardelli, I. Carnelli, A. Hilgers, D. Rodgers, Electrostatic tractor for near earth object deflection, in: 59th International Astronautical Congress.

[20] L.A. Stiles, C.R. Seubert, H. Schaub, Effective Coulomb force modeling in a space environment, in: AAS Spaceflight Mechanics Meeting, Charleston, South Carolina, Paper AAS 12.

[21] H. Schaub, J.L. Junkins, Analytical mechanics of space systems, AIAA Education Series, Reston, VA, 2nd edition, 2009.

[22] R. Mukherjee, D. Chen, Asymptotic stability theorem for autonomous systems, J. Guid. Control Dyn. 16 (1993) 961–963.

[23] N.S. Nise, Control Systems Engineering, 5th edition, John Wiley, 2008.